

heat transfer characteristics, those differences can change the simulation results significantly. Both codes adopt film model in condensation heat transfer. Comparison table of the condensation heat transfer model is presented in Table I. And the result of film thickness calculation in 3 ~ 15 MPa saturated steam

condition is presented in Table II. Condensation heat transfer coefficient of PHX is inversely proportional to film thickness. Therefore, it can be expected that PHX heat removal rate in MELCOR 2.2 will be evaluated larger than MARS-KS.

TABLE I: Comparison of Condensation Heat Transfer Model

Category	MARS-KS	MELCOR 2.2
Condensation Heat Transfer model	Film model $h_{cond.} = \frac{K_f}{\delta}, \delta = \left(\frac{3\mu_f \Gamma}{g\rho_f} \right)^{1/3}, \Gamma = \frac{\dot{m}_f}{\pi D_i}$	Film model $H_f = \max(H_{f,corr}, K_f / \delta)$ $H_{f,corr} = [K_f / (v_f / \rho_f)^2 / g]^m Nu_f$
	where, $h_{cond.}$: condensation heat transfer coefficient [$\frac{W}{m^2 \cdot K}$] K_f : fluid thermal conductivity [$\frac{W}{m \cdot K}$] δ : film thickness [m] μ_f : fluid viscosity [$\frac{kg}{m \cdot sec}$] ρ_f : fluid density [$\frac{kg}{m^3}$] Γ : liquid mass flow per unit periphery [$\frac{kg}{sec}$]	D_i : inside diameter [m] H_f : liquid film heat transfer coefficient $H_{f,corr}$: function depends on surface geometry v_f : kinematic fluid viscosity [$\frac{m^2}{sec}$] g : acceleration of gravity [$\frac{m}{sec^2}$] Nu_f : film Nusselt number

TABLE II: Result of Film Thickness Calculation

Pressure [MPa]	Film Thickness [m]	
	MARS-KS	MELCOR2.2
3	0.00187	0.00040
4	0.00205	0.00044
5	0.00212	0.00049
6	0.00223	0.00053
7	0.00233	0.00057
8	0.00243	0.00060
9	0.00253	0.00064
10	0.00263	0.00068
11	0.00272	0.00071
12	0.00282	0.00075
13	0.00292	0.00080
14	0.00302	0.00084
15	0.00313	0.00089

3. Numerical Analysis

Firstly, simplified PHX has been modeled by MARS-KS and MELCOR to compare the condensation heat transfer rate of PHX in steady-state conditions.

Secondly, SMART has been modeled in details by MARS-KS and MELCOR. Vessel including internal components, primary side, and secondary side including steam generators are modeled. In addition, PRHRS are also modeled in details. The same nodalization (e.g., same number of control volumes and sizes) has been used

3.1 Simplified PHX Model

The schematic nodalization of PHX is presented in Fig. 2. It is assumed that steam reservoir and ECT volume is infinite and non-condensable gas does not exist. The operating pressure range of PRHRS is from 3 to 15 MPa. Therefore, 13 cases are analyzed in both MARS-KS and MELCOR 2.2. Fig. 3 and Fig. 4 show the heat transfer rate and the flow rate of the PHX resulting from Fig. 2. The higher steam temperature and pressure cause the larger flow and heat removal rate of PHX. The flow rate and PHX heat removal rate in MELCOR 2.2 is evaluated larger than MARS-KS.

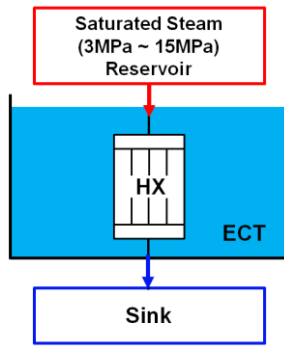


Fig. 2. Schematic Nodalization of PHX

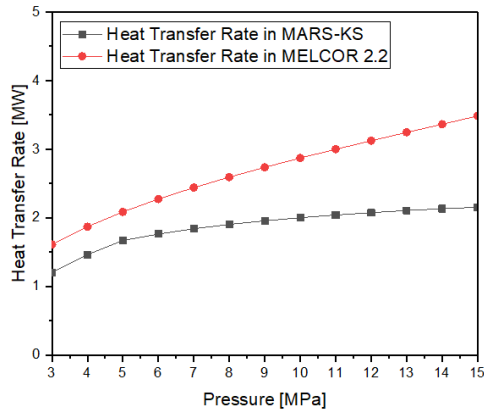


Fig. 3. Heat Removal Rate of PHX

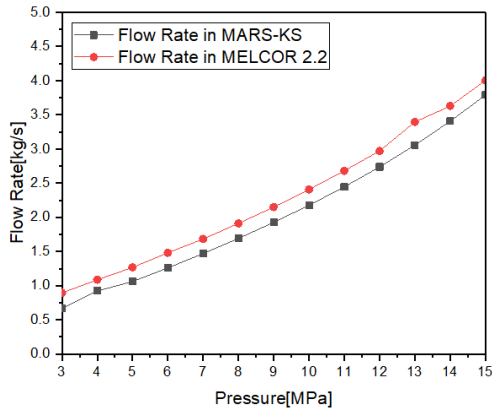


Fig. 4. Flow Rate of PHX

3.2 SMART Model

In Fig. 5, the nodalization of SMART is presented. Fig. 6 through Fig. 8 show transient behaviors of the RCS and PRHRS in a Loss of Main Feedwater (LOMF) accident. The reactor and RCP are assumed to be tripped immediately after the event initiation. The passive residual heat removal actuation signal (PRHRAS) is generated by the low feedwater flow rate at 0.0 hours, and by the PRHRAS, the main steam isolation valves and feedwater isolation valves (MSIVs/FIVs) begin to close and the PRHRS outlet isolation valves begin to open, which isolate the SGs

from turbine and connect the SGs to the PRHRS. It is assumed that 2 trains of PRHRS are available. As a result, the core temperature is not increased and the accident is not progressed further in both code analyses.

Though both codes estimate that the core would not be damaged and the accident is mitigated by 2 trains of PRHRS operation, the performance of PRHRS is evaluated quite differently. The decay heat in core would be delivered to the secondary side of SG by heat transfer via SG tubes and be removed by heat transfer in PHX. Therefore, the heat transfer is the most important mechanism in accident progression. Since MARS-KS and MELCOR have different heat transfer calculation correlations and scheme, the simulation results are differentiated.

As can be seen from the Fig. 3 and 4, the condensation heat transfer of PHX calculated by MELCOR 2.2 is larger than the one by MARS-KS. So, it is likely to expect that the MARS-KS would estimate conservatively. However, in case of LOMF as shown in Fig. 6 and 8, the PRHRS performance calculated in MARS-KS is higher than the one by MELCOR 2.2 at 72 hours. It is because the higher condensation heat transfer of PHX reduces the pressure and temperature of PRHRS rapidly at the early stage of the accident and the temperature difference between PRHRS heat source and sinks is lowered. On the other hands, in MARS-KS calculations, the natural circulation flow is established at the higher temperature difference, which incurs the lower PRHRS temperature and pressure.

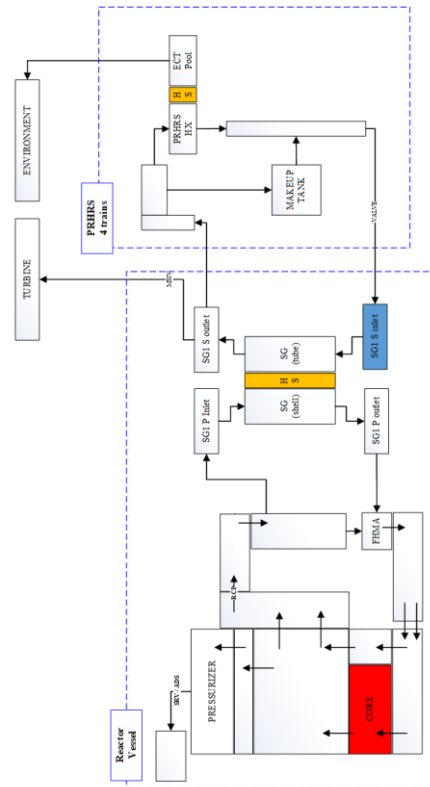


Fig. 5. SMART Nodalization of MARS-KS and MELCOR

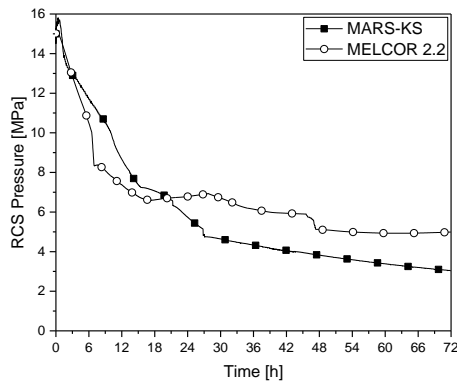


Fig. 6. LOMF – RCS Pressure

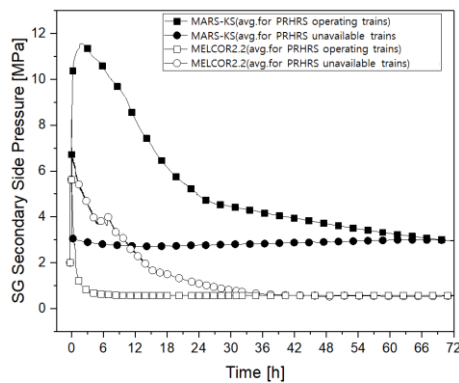


Fig. 7. LOMF – SG 2nd side Pressure

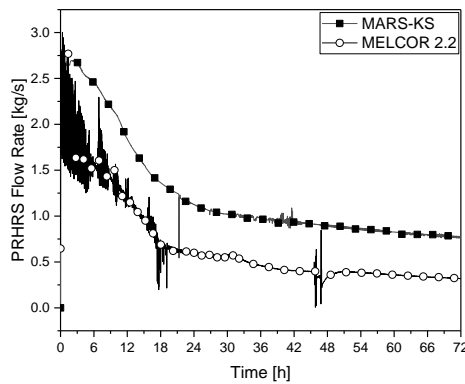


Fig. 8. LOMF – PRHRS Flow Rate

4. Conclusions

MELCOR 2.2 is compared to MARS-KS in view of SMART PRHRS analysis. Heat transfer correlations related to the major operation mechanisms of PRHRS are reviewed and numerical results are compared. It has been shown that the passive system performance would be changed sensitively according to the system operating conditions and the changed passive system performance would feedback on the system operating conditions. Estimates simply based on comparisons of heat transfer models or steady-state numerical test results would mislead the prediction on the system performance and the accident progression. To guarantee the intended functionality of the passive safety system,

special caution should be given by investigating the dynamic behavior thoroughly.

REFERENCES

- [1] Keung Koo Kim et al., “SMART: The First Licensed Advanced Integral Reactor”, *Journal of Energy and Power Engineering* 8, pp. 94-102, 2014.
- [2] Park HS, Min BY, Jung YG, et al. “Design of the VISTA ITL test facility for an integral type reactor of SMART and a post-test simulation of a SBLOCA test”, *Science and Technology of Nuclear Installations*, 2014.
- [3] Park HS, Yi SJ and Song CH, “SMR accident simulation in experimental test loop”, *Nuclear Engineering International* 58, 2013.
- [4] Bae H, Kim DE, Yi SJ, et al, “Test facility design for the validation of SMART passive safety system”, *Transactions of the Korean Nuclear Society Spring Meeting*, Korea, 2013.
- [5] Park HS, Bae H, Ryu SU, et al, “Major results from 1-train passive safety system tests for the SMART design with the SMART-TIL facility”, *Transactions of the Korean Nuclear Society Spring Meeting*, Korea, 2015.
- [6] Hwang Bae et al., “Experimental Study on SMART Steam Generator Tube Rupture Scenario using SMART-ITL”, *Transactions of the Korean Nuclear Society Autumn Meeting*, 2018.
- [7] Hee Cheol Kim et al., “Safety Analysis of SMART”, *GENES4/ANP2003*, Kyoto, Japan, 2003.
- [8] Byong Guk Jeon, “Code Validation on a Passive Safety System Test with the SMART-ITL Facility”, *Journal of Nuclear Science and Technology*, 2016.
- [9] Kim YS, Choi KY, Cho S, et al. “Second ATLAS domestic standard problem (DSP-02) for a code assessment”, *Nuclear Engineering and Technology* 45(7), 2013.
- [10] Cho YJ, Kim S, Bae BU, et al, “Assessment of condensation heat transfer model to evaluate performance of the passive auxiliary feedwater system”, *Nuclear Engineering and Technology* 45(7), 2013.
- [11] KAERI, MARS code manual volume I: code structure, system models and solution methods, KAERI/TR-2812, KAERI, 2009.
- [12] R. O. Gauntt, J.E. Cash, R. K. Cole, C. M. Erickson, L.L. Humphries, S. B. Rodriguez, and M. F. Young. MELCOR Computer Code Manuals Vol. 1 Primer and User's Guide Version 2.2, SAND2017-0876, Sandia National Laboratories, 2017.